

Winter 2-11-2013

## MUC4 overexpression augments cell migration and metastasis through EGFR family proteins in triple negative breast cancer cells.

Partha Mukhopadhyay  
*University of Nebraska Medical Center*

Imayavaramban Lakshmanan  
*University of Nebraska Medical Center, ilakshmanan@unmc.edu*

Moorthy P. Ponnusamy  
*University of Nebraska Medical Center, mpalanim@unmc.edu*

Subhankar Chakraborty  
*University of Nebraska Medical Center*

Maneesh Jain  
*University of Nebraska Medical Center, mjain@unmc.edu*

Follow this and additional works at: [https://digitalcommons.unmc.edu/com\\_bio\\_articles](https://digitalcommons.unmc.edu/com_bio_articles)  
See next page for additional authors



Part of the [Medical Biochemistry Commons](#), and the [Medical Molecular Biology Commons](#)

---

### Recommended Citation

Mukhopadhyay, Partha; Lakshmanan, Imayavaramban; Ponnusamy, Moorthy P.; Chakraborty, Subhankar; Jain, Maneesh; Pai, Priya; Smith, Lynette M.; Lele, Subodh M.; and Batra, Surinder K., "MUC4 overexpression augments cell migration and metastasis through EGFR family proteins in triple negative breast cancer cells." (2013). *Journal Articles: Biochemistry & Molecular Biology*. 61.  
[https://digitalcommons.unmc.edu/com\\_bio\\_articles/61](https://digitalcommons.unmc.edu/com_bio_articles/61)

This Article is brought to you for free and open access by the Biochemistry & Molecular Biology at DigitalCommons@UNMC. It has been accepted for inclusion in Journal Articles: Biochemistry & Molecular Biology by an authorized administrator of DigitalCommons@UNMC. For more information, please contact [digitalcommons@unmc.edu](mailto:digitalcommons@unmc.edu).

---

**Authors**

Partha Mukhopadhyay, Imayavaramban Lakshmanan, Moorthy P. Ponnusamy, Subhankar Chakraborty, Maneesh Jain, Priya Pai, Lynette M. Smith, Subodh M. Lele, and Surinder K. Batra

# MUC4 Overexpression Augments Cell Migration and Metastasis through EGFR Family Proteins in Triple Negative Breast Cancer Cells

Partha Mukhopadhyay<sup>1</sup>, Imayavaramban Lakshmanan<sup>1</sup>, Moorthy P. Ponnusamy<sup>1</sup>, Subhankar Chakraborty<sup>1</sup>, Maneesh Jain<sup>1</sup>, Priya Pai<sup>1</sup>, Lynette M. Smith<sup>2,3</sup>, Subodh M. Lele<sup>3</sup>, Surinder K. Batra<sup>1,4\*</sup>

**1** Department of Biochemistry and Molecular Biology, University of Nebraska Medical Center, Omaha, Nebraska, United States of America, **2** Department of Biostatistics, University of Nebraska Medical Center, Omaha, Nebraska, United States of America, **3** Department of Pathology and Microbiology, University of Nebraska Medical Center, Omaha, Nebraska, United States of America, **4** Eppley Institute for Research in Cancer and Allied Diseases University of Nebraska Medical Center, Omaha, Nebraska, United States of America

## Abstract

**Introduction:** Current studies indicate that triple negative breast cancer (TNBC), an aggressive breast cancer subtype, is associated with poor prognosis and an early pattern of metastasis. Emerging evidence suggests that MUC4 mucin is associated with metastasis of various cancers, including breast cancer. However, the functional role of MUC4 remains unclear in breast cancers, especially in TNBCs.

**Method:** In the present study, we investigated the functional and mechanistic roles of MUC4 in potentiating pathogenic signals including EGFR family proteins to promote TNBC aggressiveness using *in vitro* and *in vivo* studies. Further, we studied the expression of MUC4 in invasive TNBC tissue and normal breast tissue by immunostaining.

**Results:** MUC4 promotes proliferation, anchorage-dependent and-independent growth of TNBC cells, augments TNBC cell migratory and invasive potential *in vitro*, and enhances tumorigenicity and metastasis *in vivo*. In addition, our studies demonstrated that MUC4 up-regulates the EGFR family of proteins, and augments downstream Erk1/2, PKC- $\gamma$ , and FAK mediated oncogenic signaling. Moreover, our studies also showed that knockdown of MUC4 in TNBC cells induced molecular changes suggestive of mesenchymal to epithelial transition. We also demonstrated in this study, for the first time, that knockdown of MUC4 was associated with reduced expression of EGFR and ErbB3 (EGFR family proteins) in TNBC cells, suggesting that MUC4 uses an alternative to ErbB2 mechanism to promote aggressiveness. We further demonstrate that MUC4 is differentially over-expressed in invasive TNBC tissues compared to normal breast tissue.

**Conclusions:** MUC4 mucin expression is associated with TNBC pathobiology, and its knockdown reduced aggressiveness *in vitro*, and tumorigenesis and metastasis *in vivo*. Overall, our findings suggest that MUC4 mucin promotes invasive activities of TNBC cells by altering the expression of EGFR, ErbB2, and ErbB3 molecules and their downstream signaling.

**Citation:** Mukhopadhyay P, Lakshmanan I, Ponnusamy MP, Chakraborty S, Jain M, et al. (2013) MUC4 Overexpression Augments Cell Migration and Metastasis through EGFR Family Proteins in Triple Negative Breast Cancer Cells. PLoS ONE 8(2): e54455. doi:10.1371/journal.pone.0054455

**Editor:** Dhyan Chandra, Roswell Park Cancer Institute, United States of America

**Received:** November 8, 2012; **Accepted:** December 11, 2012; **Published:** February 11, 2013

This is an open-access article, free of all copyright, and may be freely reproduced, distributed, transmitted, modified, built upon, or otherwise used by anyone for any lawful purpose. The work is made available under the Creative Commons CC0 public domain dedication.

**Funding:** This work was supported by grants from the Department of Defense (BC074639, BC083295, and BC09742) and the Susan Komen Foundation (KG070826). The funders had no role in study design, data collection and analysis, decision to publish, or preparation of the manuscript.

**Competing Interests:** The authors have declared that no competing interests exist.

\* E-mail: sbatra@unmc.edu

## Introduction

Triple negative breast cancers (TNBCs) represent approximately 10–17% of all breast cancer incidents [1]. In comparison to the luminal subtypes, TNBCs are associated with poor prognosis [2], short survival, and high recurrence rates after adjuvant therapy [3]. TNBCs are associated with increased risk for visceral [4] and brain metastases, and also require more aggressive treatment. Although several therapeutic options targeting EGFR, PARP1, VEGF- $\alpha$ , Src, HDAC, and MEK are being investigated in clinical trials [5], the overall prognosis of patients with TNBC remains dismal owing to a lack of effective treatment. Thus, there is an

urgent need to investigate the underlying molecular mechanisms responsible for the aggressive nature of TNBC, and to develop targeted approaches for treatment of invasive TNBCs.

Epithelial cells produce mucins to lubricate and protect themselves from extrinsic physical and biological assaults [6]. However, aberrant expression of mucins has been reported to promote cancer development, and affects cellular growth, transformation, and invasion [7]. Aberrantly over-expressed membrane-tethered mucins, including MUC1 [8] and MUC4 [6], play diverse functional roles in several epithelial cancers, including ovarian, pancreatic [9,10], and breast [11]. We have previously demonstrated that MUC4 enhances tumorigenicity and metastasis

in pancreatic [7,12] and ovarian [10] cancer. Furthermore our studies have established that MUC4 is associated with drug resistance in pancreatic cancer [13,14]. An earlier study reported that there is a high incidence of MUC4 expression in breast cancer [15], which is associated with metastatic disease [16]. However, inadequate information is available regarding the functional role(s) of MUC4 mucin in breast cancer especially in TNBC.

In the current study, we investigated the role of MUC4 in TNBC by *in vitro* and *in vivo* functional studies, and by studying the expression of MUC4 in TNBC tissue. MUC4 potentiated oncogenic signals to promote proliferation, growth, motility, and invasiveness of TNBC cells *in vitro*, and tumorigenicity and metastasis *in vivo*. Furthermore, compared to normal breast tissues, MUC4 expression was overexpressed in invasive TNBC tissues. Thus, we propose that MUC4 mucin is a new potential target for treatment of invasive and metastatic TNBCs.

## Materials and Methods

### Cell Culture

MDA-MB-231 (HTB-26), BT-20 (HTB-19), and MDA-MB-468 (HTB-132) parental cell lines were a generous gift from Dr. Vimla Band, University of Nebraska Medical Center, Omaha, NE, USA. These cell lines are commercially available in American Type Culture Collection (ATCC) and already published in many research articles. A limited number of passages of ATCC characterized cells was maintained, tested to be free of mycoplasma contamination, and cryopreserved. All experiments were performed with cells at less than 20 passages after receipt. The  $\alpha$ -MEM media (Invitrogen, Carlsbad, CA) supplemented with 10% fetal bovine serum, 100 U/ml penicillin, 100  $\mu$ g/ml streptomycin, 2 mM L-glutamine, 10 mM HEPES (pH 7.4), and  $1 \times$  NEAA was used for maintaining MDA-MB-231 cells and also to maintain sustained MUC4 expression. After stable transfection and clone selection, control MDA-MB-231-SCR and MUC4 knockdown MDA-MB-231-shMUC4 cells were maintained in complete  $\alpha$ -MEM media with the addition of 1–3  $\mu$ g/ml puromycin.

### Stable Silencing of MUC4 using a Plasmid Construct (pSUPER-retro-puro-shMUC4)

The method of generating the shRNA construct for *in vitro* stable knockdown of MUC4 has been described previously [7]. Briefly, phoenix packaging cells were transfected with the pSUPER-retro-puro vector containing either the MUC4 shRNA insert (pSUPER-retro-puro-shMUC4) or a scrambled sequence (pSUPER-retro-puro-SCR) using FuGENE 6 (Invitrogen) following the manufacturer's protocol. Media containing infection-competent retroviruses containing supernatant were collected 48 h after transfection. Polybrene (4  $\mu$ g/mL) was added with the retroviruses to enhance the target cell infection efficiency. Cells (MDA-MB-231) were plated in 100 mm dishes at 60% confluence and infected with the retroviruses. Stable pooled populations of MDA-MB-231-SCR (control) and MDA-MB-231-shMUC4 (MUC4 knockdown) cells were generated by selection using puromycin, and levels of mRNA transcripts, expression of protein, and the phenotype of cells were analyzed. The control and MUC4 knockdown cells were used for all functional studies.

### Growth Kinetic Studies

Growth kinetics and population doubling time of control and MUC4 knockdown cells were determined as described previously [12]. Briefly, for growth curves, control and MUC4 knockdown cells were seeded at  $1 \times 10^4$  cells/well in 6-well-plate in triplicate. Viable cells of control and MUC4 knockdown populations in each

well of the 6-well plates were counted for 7 days by a viable cell counter (ViCell Coulter counter, Beckman Coulter, Inc., Brea, CA). Population doubling times of control and MUC4 knockdown cells were calculated from the number of cells growing in the log phase (96–144 h) and using the formula:  $T_d = 0.693t/\ln(N_t/N_0)$ , where t is time (in h),  $N_t$  is the cell number at time t, and  $N_0$  is the cell number at initial time.

### Colony Forming Assay

Colony forming assays were performed as described previously [17]. Briefly, colony-forming efficiency was examined 14 days after plating 250 cells/60 mm dish in quadruplicate, by staining with crystal violet (Sigma, St. Louis, MO). Colonies of  $>50 \mu$ m in size were counted using quantity One software (Bio-Rad, Richmond, CA, USA). Results are an average of 3 independent experiments.

### Assay for Anchorage Independent Growth in Soft Agar

Anchorage-independent growth assays were performed as described previously [18]. Briefly,  $2.5 \times 10^4$  cells of control and MUC4 knockdown cells were plated in 6-well plates in 1.5 mL of 0.35% low melting agarose (Sigma) in  $\alpha$ -MEM media on top of a bottom layer of 0.5% agarose in  $\alpha$ -MEM media. Plates were incubated for 2 weeks. Phase-contrast images were obtained under  $40\times$  magnification, and colonies were counted and plotted. Control and MUC4 knockdown cells were used for each experiment in triplicate. At least two independent experiments were performed.

### Immunoblot Assays

Protein extraction and immunoblotting were performed using standard procedures with control and MUC4 knockdown cells for EGFR, ErbB2, ErbB3, ErbB4,  $\beta$ -catenin, cyclin D1, CK-18, vimentin, vitronectin, ERK, FAK, and  $\beta$ -actin expression. 2% SDS-agarose gel electrophoresis was performed for MUC4 using 25  $\mu$ g protein samples under reducing conditions as described previously [19]. ErbB2 (sc-52349), ErbB3 (sc-7390), ErbB4 (sc-8050), cyclin D1(sc-718), vitronectin (sc-28929), FAK (sc-557), p-FAK (sc-7383), HSC70 (sc-7298), Sprouty 2 (sc-30049) were purchased from Santa Cruz Biotechnology, CA, US. Anti-CK-18 (K0199-21) was purchased from US Biological, MA, US; antibodies against vimentin (V-2258),  $\beta$ -actin (A-2066) were purchased from Sigma-aldrich, St. Louis, MO, US; Erk1/2 (9194); anti-p-Erk1/2 (9101) was purchased from Cell signaling, MA, US; anti-PKC $\gamma$  (ab71558) was from Abcam, Cambridge, MA, US; anti-Zonula occludens-1 (40–2300) from Invitrogen, Carlsbad, CA. EGFR (ICI). Anti-MUC4 antibodies 8G7 and 2214 were generated and characterized in our laboratory [20].  $\beta$ -catenin antibody was from kind gift Dr. Keith Johnson, UNMC, NE.

### Three-dimensional Morphogenesis Assay and Confocal Imaging

The three-dimensional Matrigel assays were performed following the method described previously [21]. Approximately,  $2.5 \times 10^3$  cells per well, as single cell suspensions, were plated onto an eight-well chamber slides on top of a polymerized layer of 100% growth factor reduced Matrigel (BD BioSciences, San Jose, CA, US), with 0.4 mL assay media containing 2% Matrigel using the overlay method [22]. Stable transfectants were cultured with puromycin. The medium was changed after every 3 days for each set. 3D structures formed by both control and MUC4 knockdown cells were quantified. Acinar-like structures were defined as regular, round structures that were clearly identified by bright

field microscopy at 20× magnification; protrusive structures were defined as those exhibiting one or more multicellular outgrowths clearly invading the surrounding Matrigel. This observation was further confirmed by staining with junctional protein zonula occludens-1 (ZO-1). Immunofluorescence microscopy was performed following a standard methodology as described previously [21].

### Quantitative Real-time Polymerase Chain Reaction

Quantitative real-time PCR was performed using standard procedures using a LightCycler 480 SYBR Green 1 Master (Roche, Germany) with specific primers as described previously [23]. The forward and reverse primers for MUC4, and  $\beta$ -actin were custom synthesized from IDT technology (Integrated DNA Technology, Coralville, IA, USA) and are listed in Table S2.

### Immunohistochemistry

Immunohistochemical analysis of tumor microarrays and sections, obtained from tumors generated by orthotopic implantation of control and MUC4 knockdown cells, was performed as described previously [24]. Briefly, after baking at 56°C overnight, the tissues were dewaxed in xylene twice for 5 min, followed by rehydration through graded ethanol. Endogenous peroxidase activity was quenched by incubating the slides with 3% hydrogen peroxide in methanol for 30 min. Antigen retrieval was performed in 0.01 M pre-heated citrate buffer (pH 6.0, 95°C) in a microwave for 15 min. Non-specific reactivity with the antibody was blocked by incubating the slides with horse serum (ImmPRESS Universal Antibody Kit, Vector Labs, Burlingame, CA, USA) for 2 h followed by the addition of the primary anti-MUC4 antibody [1:200] (Mouse monoclonal antibody 2214; 1.66 mg/ml). After overnight incubation at 4°C, the slides were washed with PBS and incubated with universal secondary antibody (ImmPRESS Universal Antibody Kit, Vector Labs) for 30 min. Staining was visualized by adding 3, 3'-diaminobenzidine solution (DAB Substrate Kit, Vector Labs). The slides were counterstained with Gill's hematoxylin (Vector Labs) and dehydrated in graded ethanol and washed with xylene. The slides were mounted with a few drops of permanent mounting medium (Permount, Fisher Scientific, Pittsburgh, PA, USA). All slides were observed under a Nikon light microscope and photographs of representative areas taken with the Q-capture Micropublisher 5.0 camera (Leeds Precision Instruments, Minneapolis, MN, USA) using the Q-capture suite software package (QImaging, Surrey, BC, Canada). The intensity of MUC4 expression was graded on a scale of 0 to 3 (0: no staining; 1+: weakly positive; 2+: moderately positive; 3+: strongly positive). The percentage of MUC4-positive cells was quantified.

### Immunofluorescence Staining and Confocal Laser Scanning Microscopy

Confocal analysis of control and MUC4 knockdown cells was performed as described previously [25]. Briefly, cells were grown onto 18 mm glass coverslips aseptically and fixed with 3.7% paraformaldehyde and permeabilized with 0.5% Triton X-100. Methanol (100%, ice chilled) was used for MUC4 staining. Next, 10% goat serum for 1 h in PBS was added to block nonspecific binding sites. The primary antibody anti-MUC4 (1.86  $\mu$ g/mL, 8G7; an antibody generated in our laboratory) was added to coverslips at 1:200, and then incubated overnight at 4°C in 1% goat serum in PBS. Alexa fluor-conjugated secondary antibody (Jackson ImmunoResearch, West Grove, PA, USA) was added at 1:1000 in 1% goat serum in PBS for 1 h. DAPI staining was done

during mounting. After washing in PBS and then water, images were captured and analyzed with a laser scanning confocal microscopy (Zeiss LSM 510 META, Carl Zeiss Microscopy GmbH, 07740 Jena, Germany).

For F-actin (filamentous actin) staining, phalloidin (fluorescent phallotoxins from Invitrogen) was used as described in the manufacturer's protocol. Briefly, cells were grown onto sterile 18 mm glass coverslips and fixed with 3.7% formaldehyde and permeabilized with 0.5% Triton X-100. Phalloidin at 1:40 in PBS was used to stain F-actin for 1 h. DAPI staining was done during mounting. Images were captured and analyzed with a laser scanning confocal microscopy (Zeiss LSM 510 META).

### Cell Cycle Analysis

Cell cycle analysis was performed by flow cytometry using standard procedures as described previously [17]. Briefly, cells were serum starved for 48 hours and re-stimulated with serum for 24 hours. After serum re-stimulation, cells were harvested with a PBS-based enzyme-free cell dissociation buffer (Invitrogen) followed by HPBS washing. MDA-MB-231-SCR and MDA-MB-231-shMUC4 cells were fixed for 1 hour in 70% ethanol, washed 3× with HPBS (pH 7.4), and resuspended in Telford reagent composed of propidium iodide (50  $\mu$ g/ml) supplemented with EDTA (90 mM), Triton X-100 (0.1%), and RNase A (1  $\mu$ g/ml). DNA content was measured using a FACScan cytometer (FACStar, Becton Dickinson, Franklin Lakes, NJ, USA). All samples were analyzed in triplicate, and the data presented are the average of the three independent experiments.

### Wound Healing and Trans-well Migration Assay

The motility assay was performed as described previously [26]. Briefly, control and MUC4 knockdown cells ( $1 \times 10^5$ /well) were seeded in 12-well plates. Cells were incubated in serum-free medium for 32–48 h prior to generating the wound by scraping with a plastic tip across the cell monolayer. Cells were incubated for 12 h and phase contrast images were recorded in ten different fields at the time of wounding (0 h) and 12 h thereafter. After 12 h, the migration of control and MUC4 knockdown cells was measured. The results presented are the average of two independent experiments. Trans-well migration assays were performed as described previously [27] using a chamber with monolayer-coated polyethylene terephthalate membranes (24-well insert, pore size of 8  $\mu$ m) for both control and MUC4 knockdown cells. The results presented are the average of three experiments.

### Cell Invasion Assay

The invasion assay was performed as described previously [28] using a chamber with Matrigel-coated membrane inserts (24-well insert, pore size of 8  $\mu$ m) for both control and MUC4 knockdown cells.

### Microarray Gene Expression Analysis

Total RNA was isolated using RNeasy Mini Kit columns as described by the manufacturer (Qiagen, Valencia, CA, US). RNA yield and purity were measured photo-metrically using nanodrop (NanoDrop 1000 spectrophotometer, Thermo Scientific, Wilmington, Delaware USA) and also in criterion gel (Bio-Rad). Spotted microarrays were used to identify differentially expressed genes between MDA-MB-231-SCR (control) and MUC4 knockdown MDA-MB-231-shMUC4 samples. After reverse transcription with SuperScript II, cDNA was transcribed and control and MUC4 knockdown samples were labeled with Cy3 and Cy5 respectively, and hybridized to HOA\_005\_0001 human OneAr-

ray DNA microarrays (Phalanx Biotech, CA, USA) containing 30,275 features probing for approximately 22,000 unique genes, according to standard procedures followed at the Microarray Core Facility of the University of Nebraska Medical Center (UNMC), Omaha, NE. A universal human reference (Stratagene, Cat: 740000, Cedar Creek, TX, US) was used for normalization. Microarrays were scanned with the GenePix 4000B Scanner (Axon Instruments, Foster City, CA, US). The Gene Expression Omnibus (GEO) accession number for our micro array data is **GSE40157**. (<http://www.ncbi.nlm.nih.gov/geo/query/acc.cgi?token=nfqldmkagcqwcr&acc=GSE40157>).

### Data Analysis and Real Time Validation

Data analysis and real time validation were performed using standard procedure as described previously [23]. Briefly, array quality control, statistical data analysis, and data visualization were performed at the University of Nebraska Medical Center using standard settings. Spot filters, background subtraction, and lowess normalization were applied prior to data analysis through BRB ArrayTools developed by Dr. Richard Simon and Amy Peng [29]. Genes were excluded if any of the spots were missing for any of the samples. Random-variance paired t-tests were used to determine those genes that were differentially expressed between control and MUC4 knockdown samples, by comparing the log Cy3 (control) and Cy5 (MUC4 knockdown) channel intensities. A significance level of 0.001 was selected to limit the false discovery rate due to multiple comparisons.

The microarray results were validated by RT-PCR. All RT-PCR reactions were performed using SYBR green based chemistry. For validation, eight of the differentially expressed genes, 4 up-regulated (COL4A5, SMAD6, CXCL1, and DUSP2) and 4 down-regulated (A100A4, PDGFRB, SOCS2, and PLCXD1), detected by microarray were selected. Validation was done using randomly selected original samples (submitted for microarray analysis) and in freshly isolated RNA from both control and MUC4 knockdown cells. Relative gene expression was determined using the 2- $\delta\delta$ CT method. Primers were custom synthesized from IDT technology and are listed in Table S2.

### In vivo Tumorigenesis and Metastasis in Nude Mice

To test tumorigenicity and metastasis, control and MUC4 knockdown cells ( $0.1 \times 10^6$ ) were orthotopically injected into the mammary fat pads of nude female mice (The Jackson Laboratory, Bar Harbor, ME, USA; and  $n=9$  for each group) and the growth of tumors was followed for 8 weeks using procedures described previously [30]. After 8 weeks, mice were euthanized according to IACUC (Institutional Animal Care and Use Committee) guidelines and checked for tumor size and metastasis. To confirm reduced metastasis by MUC4 knockdown cells,  $0.3 \times 10^6$  cells were orthotopically injected into the mammary fat pads of nude female mice ( $n=6$ ). After 8 weeks, animals were euthanized as above and checked for tumor size and metastasis. The results presented are the average of two independent experiments. Institutional Animal Care and Use Committee at University of Nebraska Medical Center has approved to proceed the above mentioned experiments. The approval number is 12-031-FC.

### Statistical Analysis

Data were analyzed using two-tailed Student's *t*-tests and two-tailed Fisher's exact tests where appropriate in Microsoft Excel 2010. The software used for the Wilcoxon rank sum test is SAS software (SAS Institute Inc., Cary, NC).  $P<0.05$  was considered statistically significant.

## Results

### MUC4 Promotes Proliferation and Growth

In a preliminary screening of breast cancer cells, we observed that the invasive MDA-MB-231 TNBC cell line expressed MUC4 when grown in  $\alpha$ -MEM media (**Figure 1A**, left lane), while non-invasive TNBC cell lines BT-20 and MDA-MB-468 [31] were MUC4 negative (data not shown). Thus, we chose MDA-MB-231 cells for further studies and generated a line with stable knockdown of MUC4 using a retroviral construct [7] to elucidate the functional significance of MUC4 in TNBC pathophysiology. A stable line generated with non-targeted scrambled shRNA (SCR) was used as control for all experiments performed in this study. Knockdown of MUC4 was confirmed by real-time PCR (data not shown), immunoblotting, and immunofluorescence analyses (**Figure 1A**). Immunoblot analysis indicated a  $\sim 95\%$  down-regulation of MUC4 at the protein level in MUC4 knockdown cells (MDA-MB-231-shMUC4) as compared with control cells (MDA-MB-231-SCR) cells.

Proliferation is an important cellular event in cancer cells. Growth kinetic analysis showed that MUC4 knockdown cells had a significantly lower ( $p=0.03$ ) proliferation rate with a doubling time of 44 hours compared with control cells, which had a doubling time of 32 hours (**Figure 1B**). Proliferation in cancer cells is mostly driven by alterations in the cell cycle or apoptosis or both [32]. Therefore, we investigated the effect of MUC4 down-regulation on cell cycle progression and apoptosis. Cell-cycle analyses revealed that 57% of control cells were in the G1 phase, with 16% of cells in the G2/M phase (**Figure 1C**, please see **Figure S1A**). In contrast, 67% of MUC4 knockdown cells were in G1, with 12% in G2M ( $p=0.005$  and  $p=0.037$ , respectively). Thus, knockdown of MUC4 resulted in the accumulation of cells in the G1 phase and inhibited their transition to G2/M via the S phase. However, no significant change in apoptosis was observed following MUC4 knockdown (**Figure S1B**). Under anchorage-dependent conditions, MUC4 knockdown cells exhibited significantly lower ( $p=0.003$ ) colony-forming ability (56%) compared with control cells (82%) (**Figure 1D**). When analyzed for anchorage-independent growth in soft agar, control cells formed numerous colonies ( $495 \pm 9$  per plate) after 2 weeks. In contrast, MUC4 knockdown cells formed significantly fewer ( $90 \pm 8$  per plate,  $p=0.001$ ) and smaller colonies, indicating that MUC4 expression contributes to a transformed phenotype of MDA-MB-231 cells (**Figure 1E**).

### MUC4 Up-regulates the EGFR Family of Proteins and Induces Downstream Signaling

EGFR plays important roles in the proliferation of TNBC [33], while MUC4 has been demonstrated to stabilize another EGFR family member, ErbB2 [25]. Thus, we studied the effect of MUC4 knockdown on the status of EGFR family members and downstream signaling. Knockdown of MUC4 resulted in reduced expression of ErbB1 (EGFR) and ErbB3, whereas ErbB4 levels remained unchanged (**Figure 2A**). This result suggests that MUC4 may use an alternative mechanism to promote aggressiveness and metastasis of TNBC cells, because ErbB2 was present at low levels in TNBC cells. Sprouty 2 enhances EGFR stability by sequestering Cbl (Casitas B-lineage Lymphoma-an E3 ubiquitin ligase), and thus inhibiting ubiquitin-mediated degradation of EGFR [34]. We observed a decreased expression of Sprouty 2 in MUC4 knockdown cells compared with control cells (**Figure 2B**). Alteration of EGFR expression by MUC4 resulted in enhanced downstream signaling *via* Erk1/2 and PKC- $\gamma$  pathways, as indicated by increased phosphorylation of Erk1/2 and increased

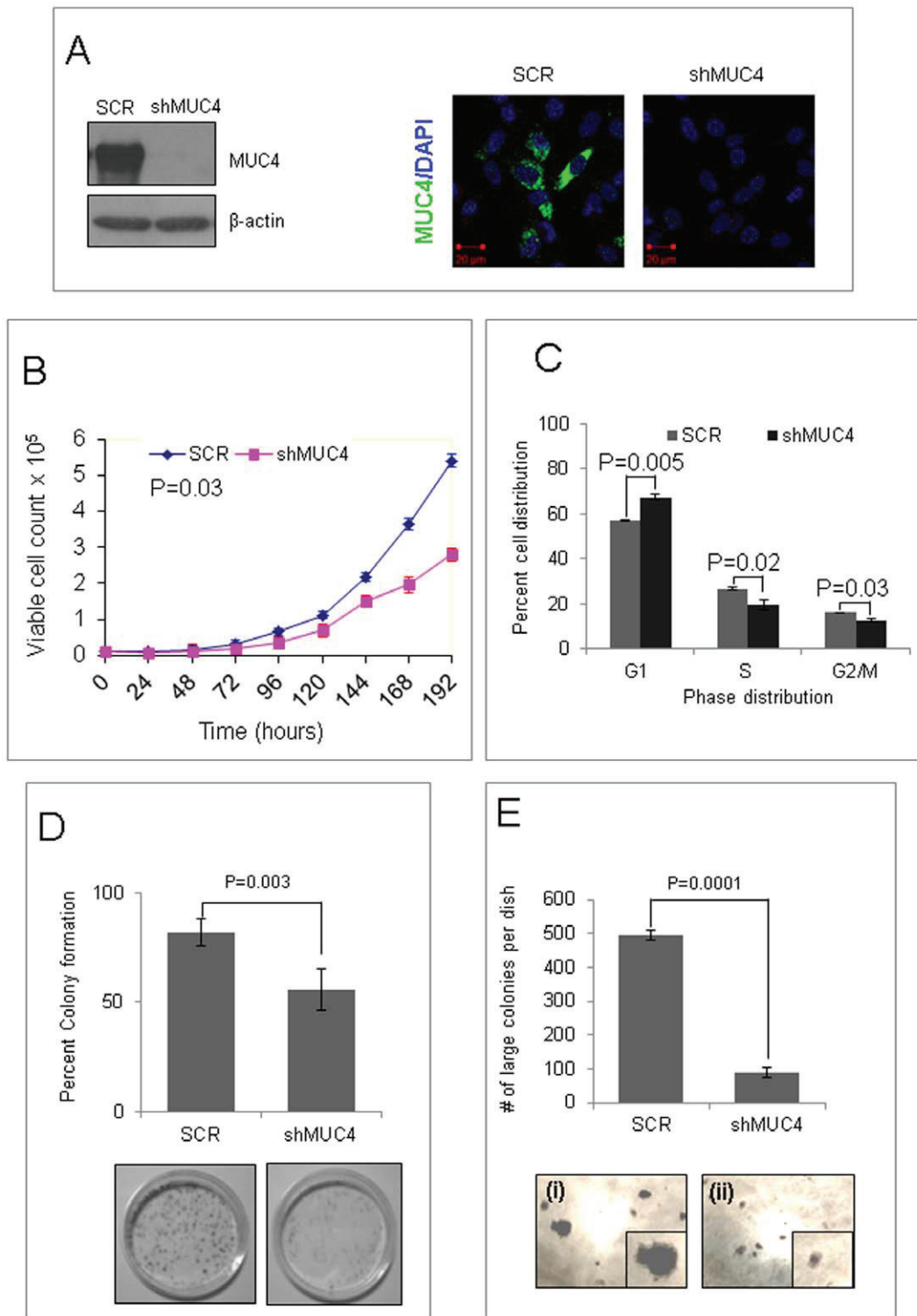


**Figure 1. MUC4 promotes proliferation and growth of MDA-MB-231 cells.** (A) Detection of MUC4 protein expression in control (MDA-MB-231-SCR) and MUC4 knockdown (MDA-MB-231-shMUC4) cells. Immunoblot showed reduced expression of MUC4 in MDA-MB-231-shMUC4 cells compared to control cells. Immunostained cells using human anti-MUC4 mouse monoclonal antibody (8G7) showed reduced expression of MUC4 in MDA-MB-231-shMUC4 cells compared to control cells. (B) In proliferation analyses, when the number of cells was plotted against the incubation period (hours), control cells showed a significantly higher proliferation rate than MUC4 knockdown cells,  $p=0.03$ . Population doubling time of control cells was less than MUC4 knockdown cells when calculated from the number of cells growing in log phase (day 2 to 6) using the formula,  $T_d = 0.693t / \ln(N_t/N_0)$ . (C) Cells, following synchronization and serum re-stimulation and stained with Telford reagent (containing propidium iodide) and analyzed by FACS, showed that the number of MUC4 knockdown cells in the G1 phase was higher than control cells suggesting the inhibition of cell cycle progression. (D) The colony forming ability of control cells was higher than MUC4 knockdown cells under anchorage-dependent conditions. After staining, colonies of  $>50 \mu\text{m}$  in size were counted using Quantity One software,  $p=0.003$ . Images of anchorage-dependent growth assays were

shown at the bottom. **(E)** The colony forming ability of control cells was higher than MUC4 knockdown cells under anchorage-independent conditions. Colonies were counted and plotted. Columns: mean of triplicates; bars: SD,  $p=0.0001$ . Phase-contrast images were recorded at  $10\times$  magnification. Microscopic images of colonies found in anchorage-independent growth assays. Higher magnification of a typical colony was shown in box on bottom right corner to emphasize a (i) big colony with migratory outer cells versus (ii) smaller and compact colonies. SCR are control and shMUC4 are MUC4 knockdown cells. All data presented are the average of 3 independent experiments. doi:10.1371/journal.pone.0054455.g001

expression of PKC- $\gamma$  in control cells (**Figure 2C**). Furthermore, MUC4 knockdown resulted in decreased expression of cyclin D1 and its upstream regulator  $\beta$ -catenin, suggesting that MUC4 augments cell cycle progression possibly *via* cyclin D1 (**Figure 2D**).

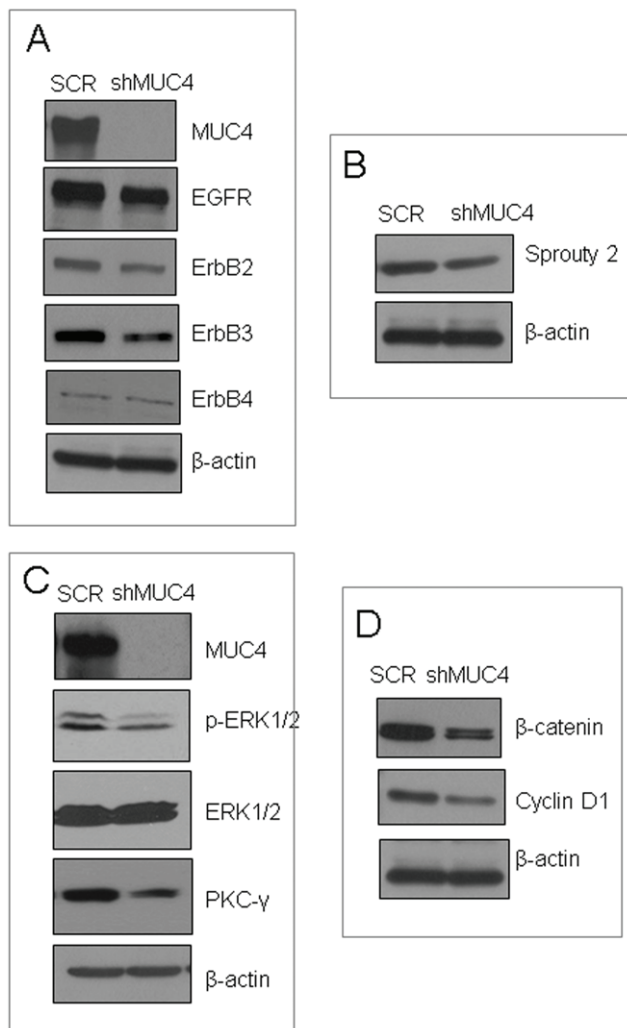


**Figure 2. MUC4 up-regulates EGFR family receptors and induces downstream Erk1/2 and PKC- $\gamma$  pathways.** (A) Immunoblot analyses showed reduced expression of EGFR, ErbB2, and ErbB3 in MUC4 knockdown cells compared with control cells. (B) Reduced expression (using immunoblot) of Sprouty 2 was detected in MUC4 knockdown cell when compared with control cells. (C) Immunoblot showed that reduced phosphorylation of Erk1/2 and expression of PKC- $\gamma$  in MUC4 knockdown cells compared with control cells.  $\beta$ -actin was used as a loading control. (D) Immunoblot analyses showed reduced expression of  $\beta$ -catenin and its target gene product cyclin D1 in MUC4 knockdown compared with control cells. doi:10.1371/journal.pone.0054455.g002

### MUC4 Enhances Migratory and Invasive Potential

In addition to enhanced proliferation, the aggressiveness of a malignant cell is determined by its migratory and invasive potential. MUC4 knockdown cells exhibited significant decrease in motility, trans-well migration, and invasion ( $p=0.01$ ,  $p=0.002$ , and  $p=0.001$ , respectively). The motility of cells, determined by their migration in the wound gap after 12 h, in the wound healing assay decreased by 18% following MUC4 knockdown (**Figure 3A**). Similarly, trans-well migration and Matrigel invasion (**Figure 3B-C**) of MUC4 knockdown cells was decreased by 58% and 65%, respectively. Since actin plays an important role in defining cell shape and orchestrating events related to cellular motility, we investigated the effect of MUC4 on actin cytoskeleton reorganization. Following cell staining with rhodamine-conjugated phalloidin, control cells exhibited more lamellipodial structures compared to MUC4 knockdown cells, which had reduced F-actin (**Figure 3D**) and decreased levels of phosphorylated (Y925) focal adhesion kinase (**Figure 3E**). These results strongly suggest that MUC4 facilitates the migratory and invasive potential of MDA-MB-231 cells by inducing the reorganization of actin filaments. Since alterations in cell motility and cytoskeleton reorganization are associated with epithelial-to-mesenchymal transition (EMT), we investigated whether MUC4 regulates EMT in MDA-MB-231 cells. MUC4 Knockdown resulted in increased expression of the epithelial marker CK-18, and decreased expression of mesenchymal markers vimentin and vitronectin (**Figure 3F**).

### MUC4 Contributes to an Altered Morphology of Colonies

Epithelial cells in the mammary gland maintain a polarized morphology, specialized cell-cell contacts, and attachment to the underlying basement membrane. The development and maintenance of this polarized structure are critical for the formation and function of mammary epithelial cells [35]. However, the pathogenesis of tumors originating from epithelial cells requires the disruption of this intact and well-organized structural design. We used a 3D Matrigel culture model [36] to determine the effect of MUC4 knockdown on the morphology of the resulting 3D structures. The control cells failed to polarize in Matrigel and formed large, disorganized colonies. MUC4 knockdown did not induce structural polarization, but resulted in the formation of more organized structures reminiscent of mammary gland acini (**Figure 4A**). Confocal imaging of 3D Matrigel structures for ZO-1, a tight junction protein, further confirmed that control cells predominantly form disorganized and larger 3D colonies in Matrigel (83%) compared with the MUC4 knockdown cells (23%;  $p=0.002$ ) (**Figure 4B**). These results indicate that MUC4 induces the transformation of MDA-MB-231 cells to a highly migratory phenotype, and that stable MUC4 knockdown partially reduces this phenomenon.

### MUC4 Promotes Tumorigenesis and Metastasis

As MUC4 knockdown was observed to augment proliferation, growth, migration, and invasion of MDA-MB-231 cells, we sought to investigate the effect of MUC4 knockdown on the tumorigenic and metastatic potential of MDA-MB-231 cells. Control and MUC4 knockdown cells were implanted orthotopically into mammary fat pads of two groups of female nude mice ( $n=9$ ).



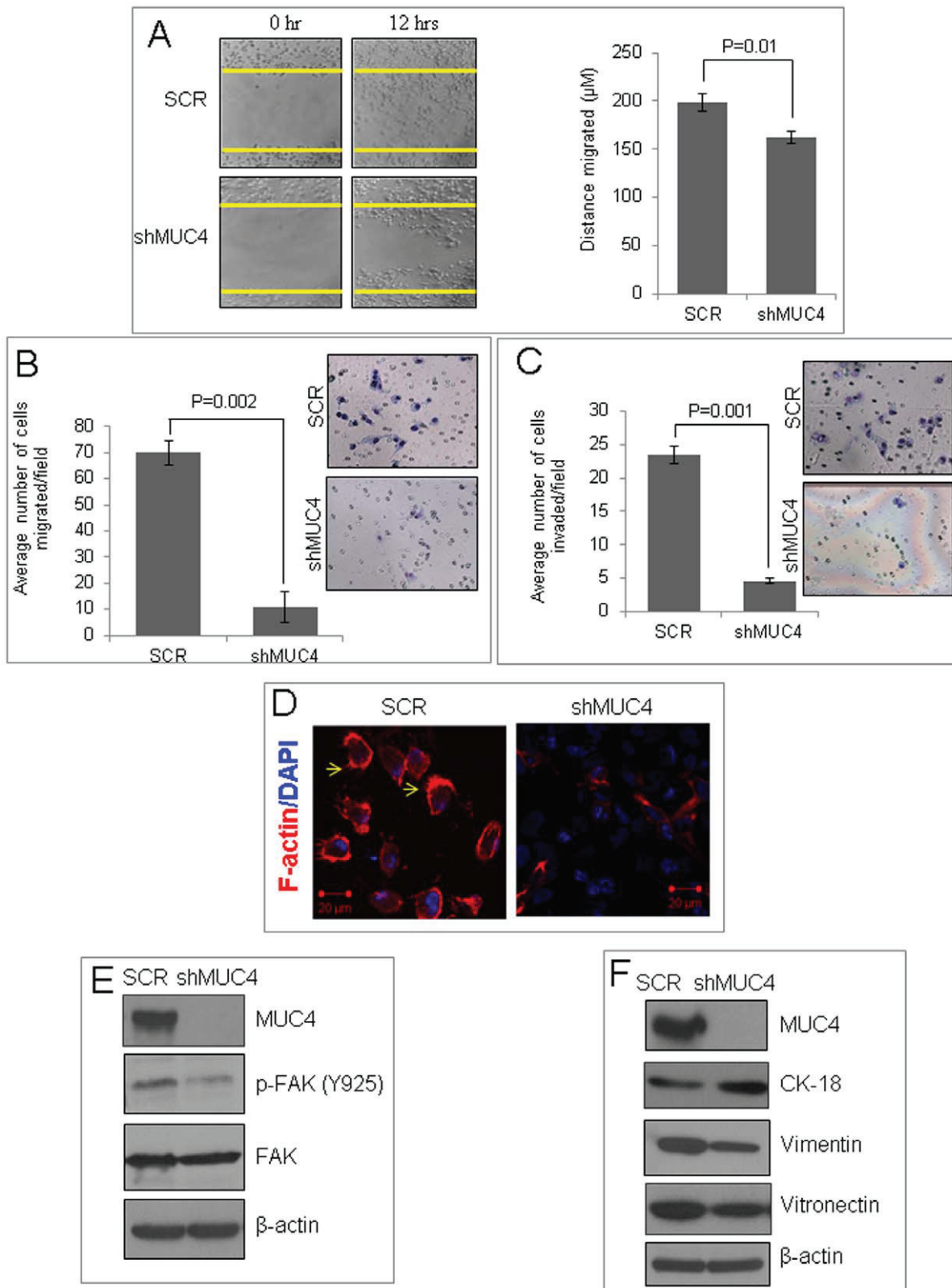


**Figure 3. MUC4 enhances migratory and invasive potential.** (A) After 24 hours serum starvation, a wound was created with a plastic tip on plates containing control or MUC4 knockdown cells. Cells were incubated in complete media for 12 hours. Motility of cells was photographed under bright-field microscopy (left, 10 $\times$  magnification). After 12 hours, the migration of control cells and MUC4 knockdown cells was measured (in  $\mu\text{m}^2$ ) using DatInF Measure setup wizard software (<http://turows.texasonline.net>). Values were calculated and plotted (right). (B and C) Control and MUC4 knockdown cells were serum starved for 48 h and seeded on non-coated or Matrigel-coated membranes for motility (B) and invasion (C) assays, respectively, and incubated for 24 h. Medium containing 10% fetal bovine serum in the lower chamber was used as a chemo-attractant. Cells that did

not migrate through the Matrigel and/or pores in the membrane were removed using a cotton swab, and cells on the other side of the membrane were stained and photographed under bright-field microscopy ( $10\times$  magnification). The number of cells that migrated and invaded was higher in control than the MUC4 knockdown cells. Data presented are the average number of cells/field for 10 fields. Columns: average of three independent experiments; bars: SE,  $p=0.002$  and  $p=0.001$ , respectively. Representative images of control and MUC4 knockdown cells were shown in both figures. **(D)** Phalloidin staining showed that visualized F-actin under a laser scanning microscope is reduced in MDA-MB-231-shMUC4 cells compared with the control cells. **(E)** Immunoblot analysis showed reduced phosphorylation of FAK in MUC4 knockdown cells compared with the control cells. **(F)** Immunoblot analysis showed reduced expression of mesenchymal markers such as vimentin and vitronectin; and increased expression of CK-18 in MUC4 knockdown cells compared to the control. doi:10.1371/journal.pone.0054455.g003

Control cells produced detectable tumors at week 3, while tumors resulting from MUC4 knockdown cells were detectable only after 5 weeks (**Figure 5A**). The tumor volume from MUC4 knockdown cells was significantly smaller ( $p=0.0001$ ) and the tumors excised at 8 weeks had markedly reduced weight, compared with tumors obtained from control cells (mean  $0.171\pm 0.05$  g in MUC4

knockdown vs.  $0.653\pm 0.07$  g in control cells) (**Figure 5B**). In addition, *in vivo* transgene expression in control cells was confirmed in excised tumors at the mRNA and protein levels (**Figure S2A-B**). Next, we determined the frequency of metastases in mice implanted with control or MUC4 knockdown cells. All mice, implanted with control cells, developed metastases to one or

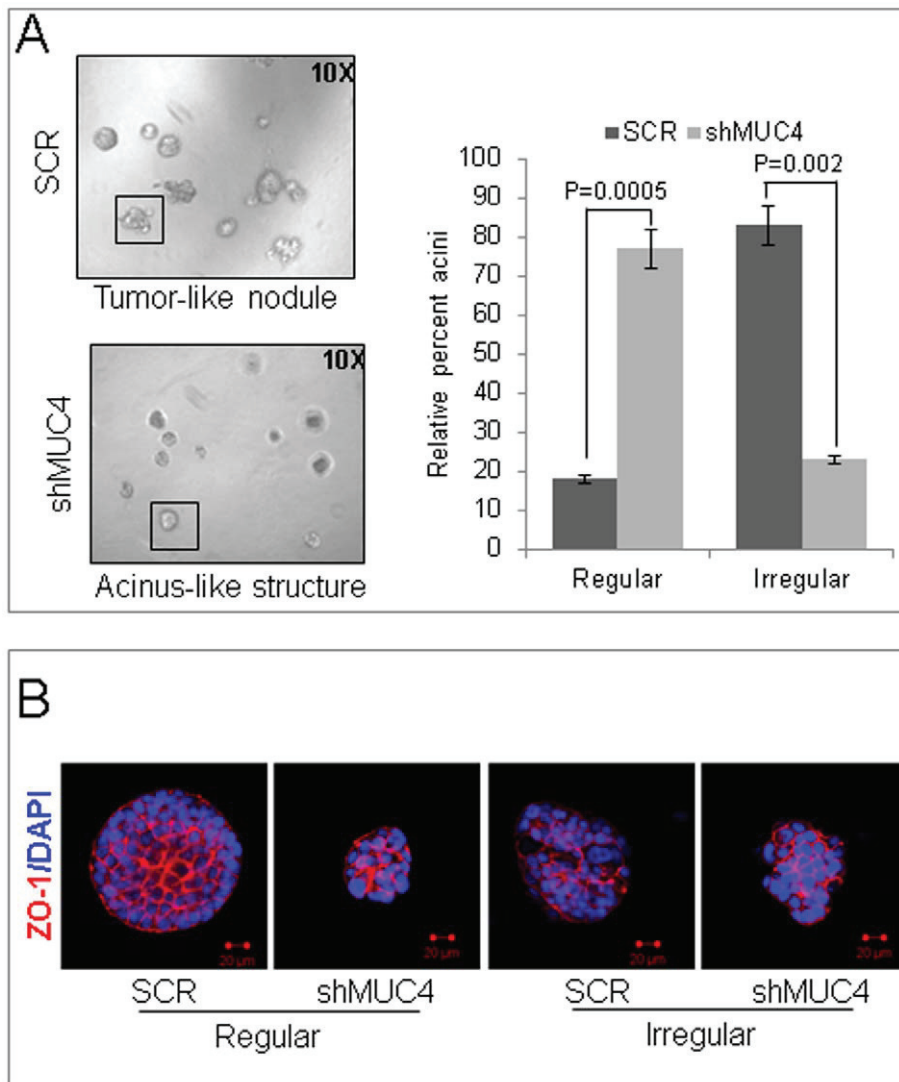


**Figure 4. MUC4 contributes to an altered phenotype.** **(A)** The control or MUC4 knockdown cells were seeded in 2% Matrigel on top of a 100% Matrigel layer, and fed with media every 3 days. After 7 days, acini-like structures were photographed under a phase-contrast microscope. The acini-like structures (examples shown in the boxes) that were regular (smooth and spherical shape) or irregular (irregular outline, multi-lobular) were counted and plotted as a percentage of the total count ( $p=0.0005$  for regular and  $p=0.002$  for irregular). A minimum of 120 structures was counted for each of control cells or MUC4 knockdown cells. Reduced irregular outline, multi-lobular and increased smooth and spherical shape colonies were found in MUC4 knock down cells when compared with control cells. **(B)** Structures were stained with the anti-ZO-1 antibody. 4,6-diamidino-2-phenylindole (DAPI) was used for nuclei staining. Optical sections ( $0.7\text{--}0.9\ \mu\text{m}$ ) were captured using a laser scanning confocal microscope. The images presented here are the central planes of the acini. Bar =  $20\ \mu\text{m}$ . doi:10.1371/journal.pone.0054455.g004

multiple sites. Metastasis was observed in 2 of nine mice of each organ such as lung, ovary, and peritoneum and; in 3 of nine of each site like mesenteric lymph nodes, and intestinal wall. In contrast no metastasis was observed in mice implanted with MUC4 knockdown cells. In an independent experiment, larger tumors were obtained by orthotopically implanting  $3 \times$  more MUC4 knockdown cells ( $0.3 \times 10^6$ ). However, these tumors, while comparable in size to the previously obtained control tumors (0.75 g), were still incapable of distant metastasis, suggesting that the differences in the metastatic potential of control and MUC4 knockdown cells is independent of the size of the primary tumor (Table S1).

### Triple Negative Breast Cancer Tissues Overexpress MUC4 Mucin

To determine the clinical relevance of MUC4 expression in TNBCs, immunohistological analyses were performed on TNBC tumor microarrays using anti-MUC4 antibody [37]. While expression of MUC4 was not detected in normal breast tissues, primary invasive TNBC tissues were found to be positive for MUC4 expression (Figure 6). A total of 35 primary tissues, and 6 normal breast tissues were examined. No expression of MUC4 was observed in the normal breast tissues (0/6, composite score  $0 \pm 0$ ), however, 54% (20/35, composite score  $2.7 \pm 1.3$ ,  $p = 0.018$ ) primary invasive TNBC tissues were found to be positive for MUC4 expression. Composite score calculated based on only 20 MUC4 positive samples was  $4.8 \pm 2.7$ ,  $p = 0.0002$ .

### MUC4-associated Gene Expression, Pathways, and Interaction Networks

We investigated alterations at transcript level following MUC4 knockdown in MDA-MB-231 cells using human genome microarray analysis. A total of 175 genes exhibited a  $>2$  fold differential expression in MUC4 knockdown cells compared with control cells. The top-scoring network of interactions among the differentially expressed genes in control versus MUC4 knockdown cells is shown along with the table that lists statistically significant enriched high-level functions (Figure S3). In agreement with the results presented in Figure 2C, the Erk1/2 and MAPK nodes were highly perturbed upon MUC4 silencing (Figure S3). Selected genes that exhibited the most differential expression in MUC4 knockdown cells are listed in Figure S4A-C. Analyses of the data revealed that several genes associated with cellular motility, proliferation, inflammatory response, and cellular signaling, were differentially regulated in MUC4 knockdown cells. Some important genes *COL4A5*, *SMAD6*, *CXCL1*, and *DUSP2* were found to be up-regulated and several other genes *A100A4*, *PDGFRB*, *CAV1*, and *CAV2* were found to be down-regulated and hence were validated (Figure 7). The results of the real time analyses were in complete agreement with the microarray data, indicating that these genes could be involved in mediating the modulation of signaling pathways by MUC4.

### Discussion

Although there is a high incidence of MUC4 expression in breast cancer [15] and a significant association with metastatic disease [16], limited information is available regarding its functional role(s) in breast cancer especially in the triple negative sub-type. We have demonstrated previously that the MUC4 promotes cell proliferation and survival by binding to the receptor tyrosine kinase ErbB2 and activating downstream signaling [10,25]. This present study represents the first effort to define

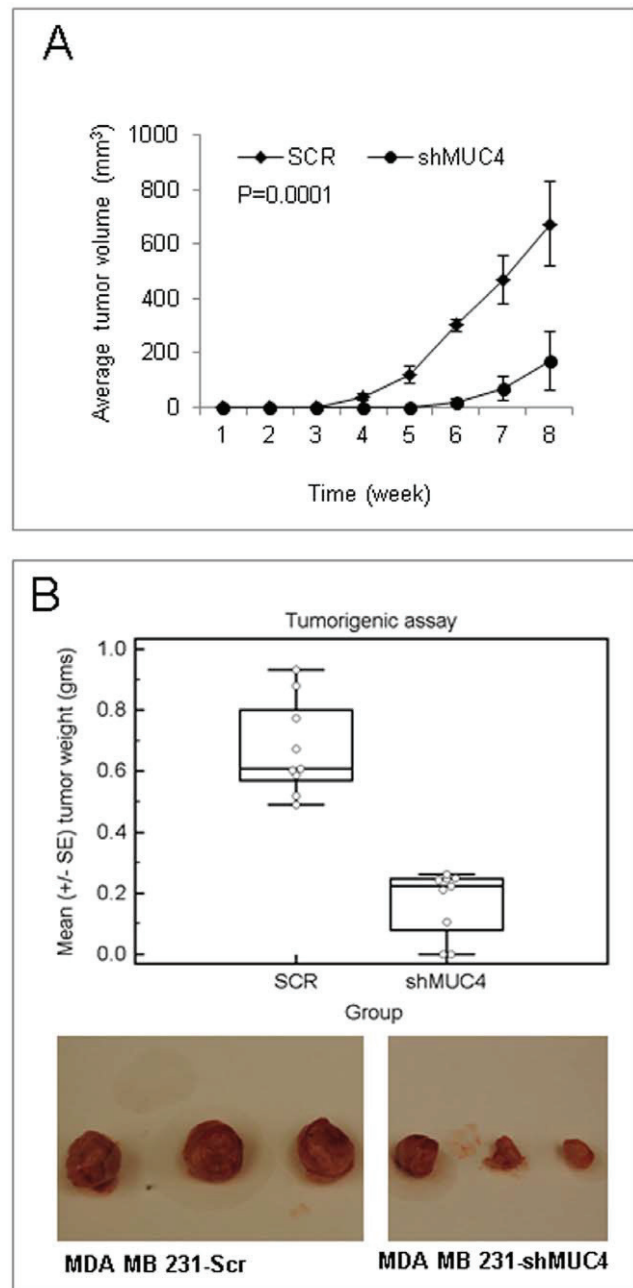


**Figure 5. MUC4 promotes growth of MDA-MB-231 xenografts.** (A) MUC4 knockdown and control cells ( $0.1 \times 10^6$  cells/animal) were orthotopically implanted in mouse mammary fat pad of each mouse (right 3<sup>rd</sup> mammary gland). Tumor volumes were calculated every week. The MUC4 knockdown cells started to grow tumors during the 5<sup>th</sup> week, but control cells started to grow tumors during the 3<sup>rd</sup> week,  $p = 0.0001$ . (B) Eight weeks after implantation, mice were sacrificed and tumors were excised and weighed. Stable silencing of MUC4 was found to decrease tumor growth,  $p = 0.0001$ . doi:10.1371/journal.pone.0054455.g005

the functional roles of human MUC4, specifically in invasive TNBC cells.

Knockdown of MUC4 in MDA-MB-231 cells resulted in a reduced growth rate, indicating that MUC4 augments cell proliferation. Previous studies from our laboratory have indicated that MUC4 augments proliferation and motility of pancreatic and

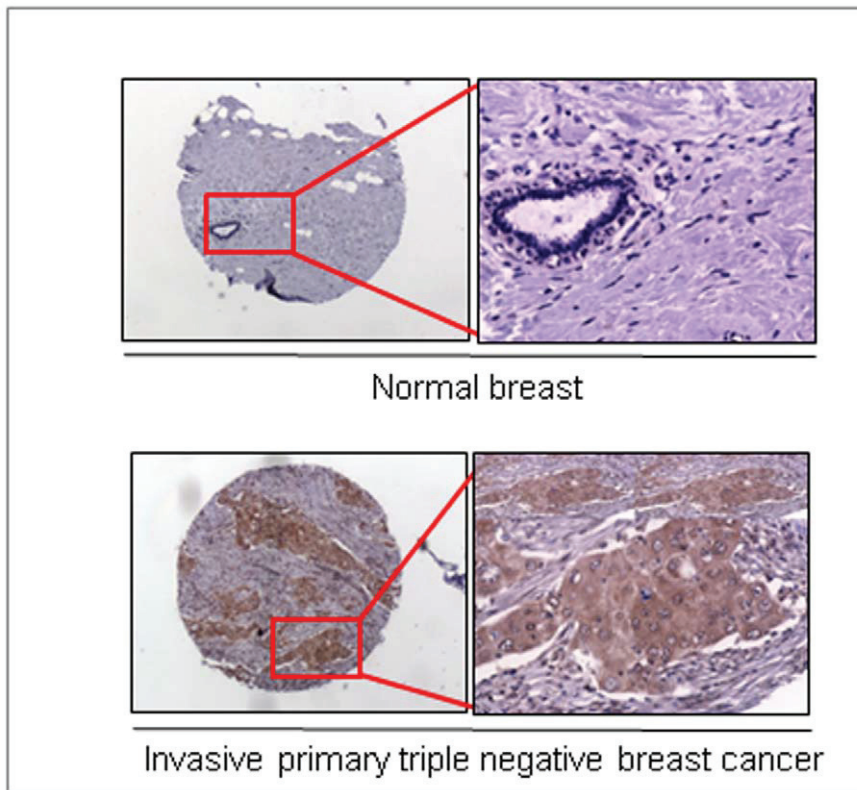


**Figure 6. Differential over-expression of MUC4 mucin in TNBC tissues compared with normal breast tissues.** Immunohistological analyses were performed using the anti-MUC4 mouse monoclonal antibody (2214, generated in our laboratory, against a sequence close to the N-terminus of human MUC4) on tumor microarrays (BR1503 and BR10010) containing normal breast and invasive TNBC tissues and observed under a Nikon light microscope. MUC4 expression in invasive primary (n=35) TNBC tissues were compared with normal breast tissue (n=6) in a set of arrays. High immune-reactivity for MUC4 was detected in invasive TNBC tissues, but not in normal breast tissues. The image presented was taken at 4× magnification, and the higher magnification images (marked with a red box) were taken at 10× magnification. doi:10.1371/journal.pone.0054455.g006

ovarian cancer cells [7,10,12,38]. In cancer cells, proliferation is mostly driven by altered cell cycle progression [32]. Increased accumulation of MUC4 knockdown cells in the G0-G1 phase suggests that MUC4-dependent signaling mediates cell cycle progression in MDA-MB-231 cells. Thus, we have shown that MUC4 augments proliferation by regulating cell cycle progression without altering apoptosis. Further investigation revealed that enhanced cell cycle progression is partly mediated by sustained expression of  $\beta$ -catenin, and thereby increased expression of cyclin D1 in control cells. MUC4 augmentation of cell cycle progression is also supported by our earlier findings in pancreatic cancer cells [7].

Among four members of the ErbB family, EGFR and ErbB2 play major roles in different types of breast cancer [39–43]. The majority of TNBCs over-express EGFR [44,45], and are therefore candidates for anti-EGFR therapies [46]. Our earlier studies demonstrated that MUC4 regulates ErbB2 expression by enhancing its stability without affecting its transcription or mRNA stability [25]. Unlike EGFR, ErbB2 is present at low levels in TNBC cells. Here, for the first time, we showed that MUC4 regulates the expression of all EGFR family receptors excluding ErbB4. This result suggests that MUC4 is using an alternative mechanism to promote the aggressiveness of TNBC cells. However, the effect of MUC4 on the levels of other receptor tyrosine kinases needs further research. Sprouty 2 attenuates EGFR ubiquitination and endocytosis, and therefore enhances Ras/ERK signaling [47]. We observed that MUC4 mucin

increased Sprouty 2 expression, and thereby potentially prevents the ubiquitin-mediated degradation of EGFR. The increased level of EGFR in MDA-MB-231 cells potentiates growth promoting downstream signaling cascades, as evident from phosphorylation of ERK1/2 and up-regulation of PKC- $\gamma$ . Further evidence of the enhanced oncogenic potential of MUC4 expressing cells was shown by their ability to undergo anchorage-dependent and -independent growth, a trait commonly used to determine the oncogenicity of cells *in vitro* [48]. Obvious increases in soft agar large colony formation were observed in control compared with MUC4 knockdown cells. Large colony formation in soft agar was inhibited by MUC4 knockdown, indicative of MUC4 dependence. Overall, analyses of soft agar colony formation together with functional indicators of oncogenesis show that MUC4 promotes oncogenic phenotypes of MDA-MB-231 cells.

Motility and invasion are also major events in the metastasis of cancer [49,50], and are associated with poor prognosis in patients with cancer. Additionally, the migratory and invasive potential of cells are typically associated with the reorganization of actin and thereby formation of lamellipodia [51]. However, the mechanisms associated with cell invasiveness remain poorly understood. Here, we demonstrate that MUC4 promotes the migratory and invasive potential of TNBC cells (Figure 3). Knockdown of MUC4 in MDA-MB-231 cells reduced migratory and invasive behaviors *in vitro* by cytoskeletal rearrangement, specifically by suppressing F-actin formation. Noticeably, MUC4 knockdown cells exhibited smaller pseudopodial projections, while control cells showed long

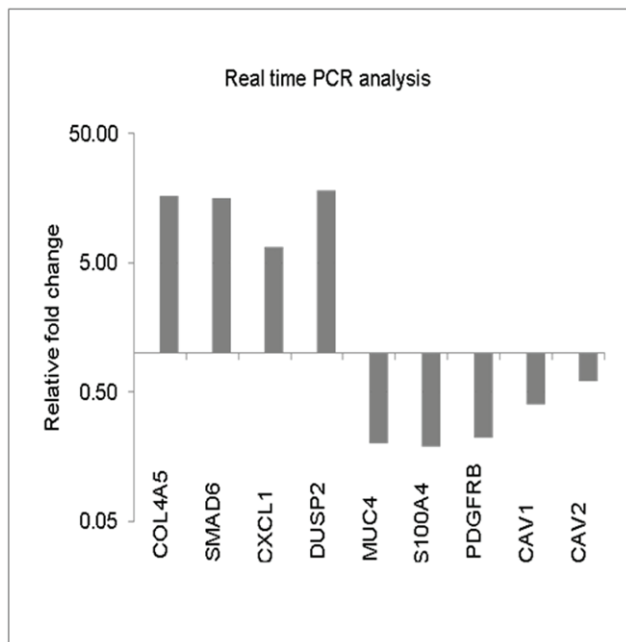


**Figure 7. MUC4-associated gene expression, pathways, and interaction networks in MDA-MB-231 cells.** Array data were validated using RT-PCR using specific primers: 20 ng mRNA from control and MUC4 knockdown cells were reverse transcribed and used for RT-PCR using MUC4 specific primers and the LightCycler SYBR Green 1 Master. The  $\beta$ -actin specific primers were used as control. CT values were calculated and plotted to verify the up-regulated and down-regulated genes.

doi:10.1371/journal.pone.0054455.g007

pseudopodial projections. The rearrangement of F-actin is associated with EMT and, therefore, increases motility [52]. Here, we showed decreased F-actin formation along with reduced motility in MUC4 knockdown cells. Furthermore, elevated expression of focal adhesions kinase (FAK) in human breast tumors has been correlated with increased malignancy and invasiveness [53]. MUC4 knockdown cells also had reduced phosphorylation of FAK, which possibly contributed to reduced motility of these cells.  $\beta$ -catenin, through its re-localization from membrane cadherin complexes to the nucleus, can act as a co-transcription factor and signaling molecule, and induces epithelial cell migration [54]. We observed decreased  $\beta$ -catenin expression in MUC4 knockdown cells, which further explains reduced motility and EMT in these cells. EMT promotes dissemination of a single carcinoma cell from the sites of primary tumors to distant organs (metastasis). In addition, EMT is required for normal mammary gland development [55] and plays a major role in breast cancer progression [56]. We observed that MUC4 knockdown resulted in increased expression of epithelial markers and decreased levels of mesenchymal markers, suggesting that MUC4 knockdown switches MDA-MB-231 cells to an epithelial from a mesenchymal phenotype. This observation is in agreement with our recent findings that showed the involvement of MUC4 in EMT in ovarian cancer cells [57]. Analyses of oncogenic behavior using biologically relevant and sensitive 3D Matrigel cultures showed that MUC4 expression in MDA-MB-231 contributes to their oncogenic potential. Although MUC4 knockdown did not induce structural polarization, organized structures reminiscent of mammary gland acini did appear. The process of metastasis is a complex phenomenon regulated by many components that facilitate the detachment of tumor cells from primary tumors to

secondary sites [49]. Our results indicate that MUC4 may potentiate the metastatic behavior of TNBC cells by inducing cytoskeletal rearrangement. The decreased proliferation rate, motility, and invasive potential observed *in vitro* following MUC4 knockdown resulted in reduced tumorigenicity and metastatic potential *in vivo*, when control and MUC4 knockdown cells were orthotopically implanted in mice. This strongly indicates that MUC4 is associated with the oncogenicity of MDA-MB-231 cells. Our experimental findings are in agreement with the expression profile of MUC4 in a small set of clinical TNBC samples. We observed that MUC4 is over-expressed in invasive TNBC tissues, but not expressed in normal breast tissues. These preliminary studies provide a strong rationale to undertake a future study in a larger sample set to determine the association of MUC4 with TNBC and other breast cancer sub-types. Taken together these findings suggest an important role for MUC4 in tumorigenesis and metastasis of TNBCs.

To further understand MUC4-mediated oncogenic signaling pathways, we studied global alterations in gene expression. Detailed analyses of microarray data further support the concept that MUC4 confers oncogenic potential to MDA-MB-231 cells. The top-scoring network of interactions (Figure S3) among the differentially expressed genes in control versus MUC4 knockdown cells involved Erk1/2, which is in complete agreement with the reduced levels of phosphorylated Erk1/2 observed in the immunoblotting experiments (Figure 2C). Moreover, we observed statistically significant changes in high-level cellular functions (Figure S3) including metastasis (22 genes), apoptosis (15 genes), tumorigenesis (12 genes), cell movement (17 genes), proliferation (29 genes), disassembly of focal adhesions (6 genes), and disassembly of actin filaments (7 genes). In addition, knockdown of MUC4 up-regulated membrane components such as type IV collagen (COL4A5), an antagonist of signaling by TGF- $\beta$  type 1 receptor super family members (SMAD6). Knockdown of MUC4 also up-regulated DUSP2, a dual phosphatase kinase, and thereby down-regulated mitogenic signal transduction by dephosphorylating both Thr and Tyr residues on Erk1/2, and agrees well with our immunoblotting data (Figure 2C). Furthermore, MUC4 knockdown up-regulated CXCL1, which is a ligand of CXCR1 and CXCR2. Controlling the levels of cytokines including CXCL1 is important for controlling immune cell infiltration, and ultimately *in vivo* tumor growth [58]. The effects of increased CXCL in the current study warrant further research.

The expression of S100A4, PDGFR, CAV1, CAV2, and many other genes was down-regulated in MUC4 knockdown cells. The S100A4 protein functions in motility, invasion, and tubulin polymerization of many cell types [59]. Chromosomal abnormalities and altered expression of S100A4 have been implicated in tumor metastasis [60]. The binding of ligands (PDGF- $\alpha$ , - $\beta$ , - $\gamma$ , and - $\delta$ ) activates the intracellular kinase activity of PDGFR, and initiates intracellular signaling through the MAPK, PI3-K, and PKC- $\gamma$  pathways. The down-regulation of PKC- $\gamma$  upon MUC4 knockdown is in agreement with our western blot data (Figure 2C). Caveolin expression is elevated in breast cancer and associated with both primary and metastatic breast cancer [61]. CAV1 (caveolin-1), has been identified as a marker associated with a basal-like phenotype in both hereditary and sporadic breast cancer [62], and has been proposed to play a role in intracellular cholesterol trafficking [63]. A schematic of the overall study performed indicates several pathways of involvement of MUC4 in the pathogenesis of invasive TNBCs (Figure 8). Altogether, these results suggest that MUC4 modulates multiple signaling pathways that confer aggressiveness to MDA-MB-231 cells.

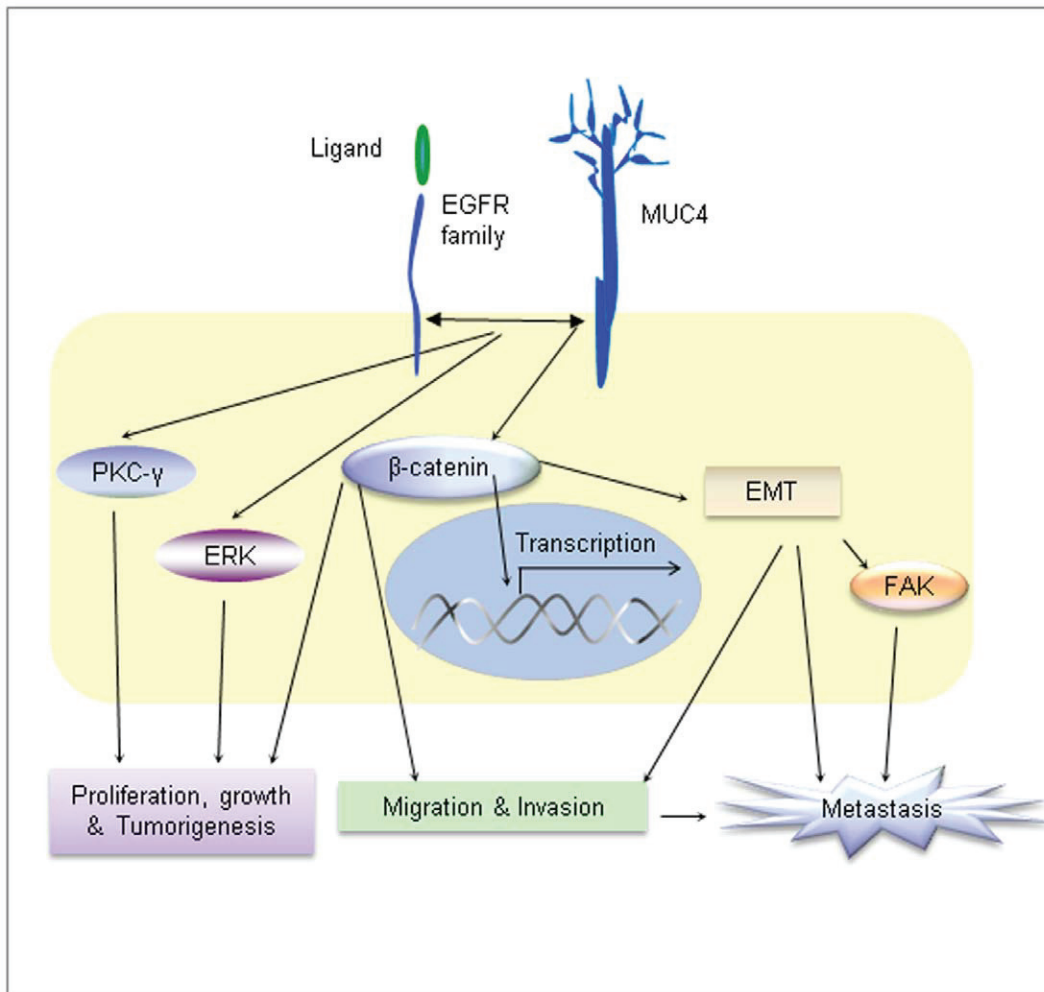


**Figure 8. A schematic diagram showing the contribution of MUC4 in the overall aggressiveness of TNBC cells.** MUC4 maintains the sustained expression of EGFR family proteins and thereby potentiates downstream signaling events mediated through the PKC- $\gamma$  and Erk1/2 signaling. MUC4 maintains sustained expression of  $\beta$ -catenin, which induces proliferation, tumorigenesis, migration, invasion, and metastasis. doi:10.1371/journal.pone.0054455.g008

## Conclusions

In conclusion, we have shown for the first time that MUC4 promotes TNBC cell invasive activity through EGFR family protein (EGFR, ErbB2 and ErbB3) and its downstream signaling (Figure 8). We have also shown that MUC4 is differentially over-expressed in primary and metastatic TNBC tissues compared with normal breast tissues. Therefore, MUC4 could be a new potential target for the treatment of invasive TNBCs.

## Supporting Information

**Figure S1 (A) Histograms of cell cycle analyses of control and MUC4 knockdown cells.** (B) Histograms of apoptosis assays of control and MUC4 knockdown cells. (TIF)

**Figure S2 MUC4 down-regulation maintained in a tumor generated by the orthotopic implantation of MDA-MB-231-shMUC4 cells in mammary fat pads of nude mice.** (A) Real-time PCR analysis of tumor samples. A total of 20 ng mRNA from tumors was reverse transcribed and used for real-time-PCR using MUC4 specific primers and SYBR green master mix. The GAPDH specific primers were used as control.

CT values were calculated and plotted. (B) Immunoblot analysis of tumor samples. A total of 50  $\mu$ g of protein from tumors was immunoblotted using 8G7 anti-MUC4 monoclonal antibody. (TIF)

**Figure S3 The top-scoring network of interactions among the differentially expressed genes in control versus MUC4 knockdown cells.** The table lists statistically significant enriched high-level cellular functions. (TIF)

**Figure S4 Regulated mRNAs in MDA-MB-231 cells, after knockdown of MUC4, using human genome array analysis.** (A) BRB-Arraytools hierarchical clustering of genes with large fold-change. (B) Names and average log fold-change values of selected down-regulated genes. (C) Names and average log fold-change values of selected up-regulated genes. (\*) real-time PCR validated genes. (TIF)

**Table S1 Metastatic spread in nude mice when MUC4 knockdown (MDA-MB-231-shMUC4) cells were implanted ( $0.3 \times 10^6$  cells) into the right 3<sup>rd</sup> mammary fat**

**pad.** No metastasis was detected in any mice injected ( $n = 6$ ) with MDA-MB-231-shMUC4 cells. (TIF)

**Table S2 List of primers that were used for real-time PCR analysis and validation of microarray data.** (TIF)

## Acknowledgments

The authors wish to thank Kavita Mallya for their technical assistance, the Microarray Core Facility for gene expression analysis, Cell Sorting Facilities for cell cycle/apoptosis analysis, and the Confocal Facility for imaging assistance. We thank Dr. Parmender Mehta for the valuable support in providing cell biology reagents and antibodies. The authors

## References

- Reis-Filho JS, Tutt AN (2008) Triple negative tumours: a critical review. *Histopathology* 52: 108–118.
- Nofech-Mozes S, Trudeau M, Kahn HK, Dent R, Rawlinson E, et al. (2009) Patterns of recurrence in the basal and non-basal subtypes of triple-negative breast cancers. *Breast Cancer Res Treat* 118: 131–137.
- Kaplan HG, Malmgren JA, Atwood M (2009) T1N0 triple negative breast cancer: risk of recurrence and adjuvant chemotherapy. *Breast J* 15: 454–460.
- Liedtke C, Mazouni C, Hess KR, Andre F, Tordai A, et al. (2008) Response to neoadjuvant therapy and long-term survival in patients with triple-negative breast cancer. *J Clin Oncol* 26: 1275–1281.
- Fong PC, Boss DS, Yap TA, Tutt A, Wu P, et al. (2009) Inhibition of poly(ADP-ribose) polymerase in tumors from BRCA mutation carriers. *N Engl J Med* 361: 123–134.
- Chaturvedi P, Singh AP, Batra SK (2008) Structure, evolution, and biology of the MUC4 mucin. *FASEB J* 22: 966–981.
- Chaturvedi P, Singh AP, Moniaux N, Senapati S, Chakraborty S, et al. (2007) MUC4 mucin potentiates pancreatic tumor cell proliferation, survival, and invasive properties and interferes with its interaction to extracellular matrix proteins. *Mol Cancer Res* 5: 309–320. 1541–7786.
- Singh PK, Hollingsworth MA (2006) Cell surface-associated mucins in signal transduction. *Trends Cell Biol* 16: 467–476.
- Bafna S, Singh AP, Moniaux N, Eudy JD, Meza JL, et al. (2008) MUC4, a multifunctional transmembrane glycoprotein, induces oncogenic transformation of NIH3T3 mouse fibroblast cells. *Cancer Res* 68: 9231–9238.
- Ponnusamy MP, Singh AP, Jain M, Chakraborty S, Moniaux N, et al. (2008) MUC4 activates HER2 signalling and enhances the motility of human ovarian cancer cells. *Br J Cancer* 99: 520–526.
- Mukhopadhyay P, Chakraborty S, Ponnusamy MP, Lakshmanan I, Jain M, et al. (2011) Mucins in the pathogenesis of breast cancer: implications in diagnosis, prognosis and therapy. *Biochim Biophys Acta* 1815: 224–240.
- Singh AP, Moniaux N, Chauhan SC, Meza JL, Batra SK (2004) Inhibition of MUC4 expression suppresses pancreatic tumor cell growth and metastasis. *Cancer Res* 64: 622–630.
- Bafna S, Kaur S, Momi N, Batra SK (2009) Pancreatic cancer cells resistance to gemcitabine: the role of MUC4 mucin. *Br J Cancer* 101: 1155–1161.
- Mimeault M, Johansson SL, Senapati S, Momi N, Chakraborty S, et al. (2010) MUC4 down-regulation reverses chemoresistance of pancreatic cancer stem/progenitor cells and their progenies. *Cancer Lett* 295: 69–84.
- Rakha EA, Boyce RW, bd El-Rehim D, Kurien T, Green AR, et al. (2005) Expression of mucins (MUC1, MUC2, MUC3, MUC4, MUC5AC and MUC6) and their prognostic significance in human breast cancer. *Mod Pathol* 18: 1295–1304.
- Workman HC, Miller JK, Ingalla EQ, Kaur RP, Yamamoto DI, et al. (2009) The membrane mucin MUC4 is elevated in breast tumor lymph node metastases relative to matched primary tumors and confers aggressive properties to breast cancer cells. *Breast Cancer Res* 11: R70.
- Dixit M, Yang JL, Poirier MC, Price JO, Andrews PA, et al. (1997) Abrogation of cisplatin-induced programmed cell death in human breast cancer cells by epidermal growth factor antisense RNA. *J Natl Cancer Inst* 89: 365–373.
- Masuda A, Kondo M, Saito T, Yatabe Y, Kobayashi T, et al. (1997) Establishment of human peripheral lung epithelial cell lines (HPL1) retaining differentiated characteristics and responsiveness to epidermal growth factor, hepatocyte growth factor, and transforming growth factor beta1. *Cancer Res* 57: 4898–4904.
- Moniaux N, Varshney GC, Chauhan SC, Copin MC, Jain M, et al. (2004) Generation and characterization of anti-MUC4 monoclonal antibodies reactive with normal and cancer cells in humans. *J Histochem Cytochem* 52: 253–261.
- Jain M, Venkatraman G, Moniaux N, Kaur S, Kumar S, et al. (2011) Monoclonal antibodies recognizing the non-tandem repeat regions of the human mucin MUC4 in pancreatic cancer. *PLoS One* 6: e23344.
- Debnath J, Muthuswamy SK, Brugge JS (2003) Morphogenesis and oncogenesis of MCF-10A mammary epithelial acini grown in three-dimensional basement membrane cultures. *Methods* 30: 256–268.

would also like to thank Dr. James D Eudy of the Department of Genetics, Cell Biology and Anatomy, UNMC for the generous help with IN-GENUITY pathway analysis. We also thank Janice A. Taylor and James R. Talaska of the confocal laser scanning microscope core facility at the UNMC, for their support.

**Note:** The Gene Expression Omnibus (GEO) accession number for our micro array data is **GSE40157**.

Link: <http://www.ncbi.nlm.nih.gov/geo/query/acc.cgi?token=nfqldmkagcqwcr&acc=GSE40157>

## Author Contributions

Conceived and designed the experiments: PM SKB. Performed the experiments: PM SC MJ MPP IL PP. Analyzed the data: LS SL. Wrote the paper: PM SKB.

44. Foulkes WD, Metcalfe K, Hanna W, Lynch HT, Ghadirian P, et al. (2003) Disruption of the expected positive correlation between breast tumor size and lymph node status in BRCA1-related breast carcinoma. *Cancer* 98: 1569–1577.
45. van de Rijn M, Perou CM, Tibshirani R, Haas P, Kallioniemi O, et al. (2002) Expression of cytokeratins 17 and 5 identifies a group of breast carcinomas with poor clinical outcome. *Am J Pathol* 161: 1991–1996.
46. Siziopikou KP, Cobleigh M (2007) The basal subtype of breast carcinomas may represent the group of breast tumors that could benefit from EGFR-targeted therapies. *Breast* 16: 104–107.
47. Wong ES, Fong CW, Lim J, Yusoff P, Low BC, et al. (2002) Sprouty2 attenuates epidermal growth factor receptor ubiquitylation and endocytosis, and consequently enhances Ras/ERK signalling. *EMBO J* 21: 4796–4808.
48. Freedman VH, Shin SI (1974) Cellular tumorigenicity in nude mice: correlation with cell growth in semi-solid medium. *Cell* 3: 355–359.
49. Hanahan D, Weinberg RA (2000) The hallmarks of cancer. *Cell* 100: 57–70.
50. Stetler-Stevenson WG, Aznavoorian S, Liotta LA (1993) Tumor cell interactions with the extracellular matrix during invasion and metastasis. *Annu Rev Cell Biol* 9: 541–573.
51. Yamaguchi H, Wyckoff J, Condeelis J (2005) Cell migration in tumors. *Curr Opin Cell Biol* 17: 559–564.
52. Wicki A, Lehenbre F, Wick N, Hantusch B, Kerjaschki D, et al. (2006) Tumor invasion in the absence of epithelial-mesenchymal transition: podoplanin-mediated remodeling of the actin cytoskeleton. *Cancer Cell* 9: 261–272.
53. Cance WG, Harris JE, Iacocca MV, Roche E, Yang X, et al. (2000) Immunohistochemical analyses of focal adhesion kinase expression in benign and malignant human breast and colon tissues: correlation with preinvasive and invasive phenotypes. *Clin Cancer Res* 6: 2417–2423.
54. Muller T, Choidas A, Reichmann E, Ullrich A (1999) Phosphorylation and free pool of beta-catenin are regulated by tyrosine kinases and tyrosine phosphatases during epithelial cell migration. *J Biol Chem* 274: 10173–10183.
55. Simian M, Hirai Y, Navre M, Werb Z, Lochter A, et al. (2001) The interplay of matrix metalloproteinases, morphogens and growth factors is necessary for branching of mammary epithelial cells. *Development* 128: 3117–3131.
56. Wiseman BS, Werb Z (2002) Stromal effects on mammary gland development and breast cancer. *Science* 296: 1046–1049.
57. Ponnusamy MP, Lakshmanan I, Jain M, Das S, Chakraborty S, et al. (2010) MUC4 mucin-induced epithelial to mesenchymal transition: a novel mechanism for metastasis of human ovarian cancer cells. *Oncogene* 29: 5741–5754.
58. Roland CL, Lynn KD, Toombs JE, Dincean SP, Udugamasooriya DG, et al. (2009) Cytokine levels correlate with immune cell infiltration after anti-VEGF therapy in preclinical mouse models of breast cancer. *PLoS One* 4: e7669.
59. Helfman DM, Kim EJ, Lukanidin E, Grigorian M (2005) The metastasis associated protein S100A4: role in tumour progression and metastasis. *Br J Cancer* 92: 1955–1958.
60. Ilg EC, Schafer BW, Heizmann CW (1996) Expression pattern of S100 calcium-binding proteins in human tumors. *Int J Cancer* 68: 325–332.
61. Yang G, Truong LD, Timme TL, Ren C, Wheeler TM, et al. (1998) Elevated expression of caveolin is associated with prostate and breast cancer. *Clin Cancer Res* 4: 1873–1880.
62. Pinilla SM, Honrado E, Hardisson D, Benitez J, Palacios J (2006) Caveolin-1 expression is associated with a basal-like phenotype in sporadic and hereditary breast cancer. *Breast Cancer Res Treat* 99: 85–90.
63. Frank PG, Cheung MW, Pavlides S, Llaverias G, Park DS, et al. (2006) Caveolin-1 and regulation of cellular cholesterol homeostasis. *Am J Physiol Heart Circ Physiol* 291: H677–H686.



Copyright of PLoS ONE is the property of Public Library of Science and its content may not be copied or emailed to multiple sites or posted to a listserv without the copyright holder's express written permission. However, users may print, download, or email articles for individual use.